Optik - International Journal for Light and Electron Optics 251 (2022) 168245

Contents lists available at ScienceDirect

Optik - International Journal for Light and Electron Optics

journal homepage: www.elsevier.com/locate/ijleo

Original research article

# Generation of low-complexity power-efficient IR-UWB waveforms

Samy S. Soliman [a,b], Mohamed Shehata [a], Hassan Mostafa [a,c,*]

[a] Electronics and Electrical Communications Engineering Department, Faculty of Engineering, Cairo University, Giza 12613, Egypt
[b] University of Science and Technology, Communications and Information Engineering Program, Zewail City of Science, Technology and Innovation, October Gardens, 6th of October, Giza 12578, Egypt
[c] University of Science and technology, Nanotechnology and Nanoelectronics Engineering Program, Zewail City of Science, Technology and Innovation, October Gardens, 6th of October, Giza 12578, Egypt

ARTICLE INFO

*Keywords:*
Impulse radio
Gaussian waveform
Power efficiency
Sech waveform
Ultra-wide band

ABSTRACT

In this paper, a low-complexity approach is proposed for the generation of power efficient impulse radio ultra-wide band (IR-UWB) waveforms. The proposed approach relies on the optimization of the pulse width to achieve the highest power efficiency while maintaining FCC-compliant pulse shapes. Analytical expressions are developed for the power efficiency of widely adopted UWB waveforms, namely Gaussian and sech basis waveforms. The proposed approach is verified analytically and compared to results obtained through other approaches in the literature. It is shown that using as low as a single first order derivative Gaussian or sech basis waveform, with optimized pulse width can result in power efficiency as high as 85%, an efficiency that is achieved by other approaches using linear combinations of as much as 33 basis waveforms. This represents the low-complexity advantage of the proposed approach, which makes it more practical for implementation.

## 1. Introduction

Ultra-wide band (UWB) signals are extremely power limited due to the very low spectral constraints imposed on their power spectral densities (PSDs) by the Federal Communications Committee (FCC) [1]. In impulse radio UWB (IR-UWB) signaling, such low power levels are emitted in the form of finite-energy packets, carried by ultrashort waveforms, in the range of nanoseconds or picoseconds. In practice, the generated IR-UWB waveforms are often amplitude and/or time-scaled single order derivatives of Gaussian and hyperbolic secant (sech) basis functions such as monocycles, doublets [2–8], and higher order derivatives [9].

According to [10], various IR-UWB waveforms, having different spectral characteristics, are obtained by varying one or more of the parameters of the basis functions such as their amplitudes, delays, temporal widths, and/or their derivative orders. Inspired by this principle, numerous IR-UWB waveform design approaches have been proposed based on carefully designed linear combinations of spectrally heterogeneous single derivative order waveforms. These approaches aim at improving the power efficiency of single derivative order IR-UWB waveforms, while complying to the FCC spectral constraints over the entire spectrum. For example, the authors in [11] have proposed the synthesis of power efficient and FCC compliant IR-UWB waveforms by linearly combining an orthogonal set of uniformly delayed $L$ Gaussian monocycle pulses using an $L$-taps finite impulse response (FIR) filter with optimized tap coefficients. Moreover, it has been proven in [11] that the power efficiency of the synthesized waveform increases with increasing the number of FIR filter taps. The efficiency of the linear combination design approach using FIR filters has been supported by many experimental evidences.

* Corresponding author at: Electronics and Electrical Communications Engineering Department, Faculty of Engineering, Cairo University, Giza 12613, Egypt.
*E-mail addresses:* samy.soliman@cu.edu.eg (S.S. Soliman), hmostafa@staff.cu.edu.eg (H. Mostafa).

https://doi.org/10.1016/j.ijleo.2021.168245
Received 11 July 2020; Received in revised form 16 August 2021; Accepted 27 October 2021
Available online 2 December 2021

In other work, the authors of [12] have experimentally demonstrated the generation of an IR-UWB waveform with power efficiency as high as 75.1% by applying a sech basis function to a 30-taps all-optical FIR filter, followed by an optical fiber-based transmission chain. However, the generation of more complicated and consequently, more power efficient, IR-UWB waveforms has been limited by the implementation complexity of the all-optical FIR filter as well as the extremely random phase noise, which increases with increasing the system complexity due to the uncontrollable imperfections in the fabrication process [12]. Therefore, to limit the impact of the phase noise, the design in [12] has been refined later in [13] by confining the number of the FIR filter taps to only eight, while including the frequency response of a combined optical and wireless transmission link. Although a theoretical optimum power efficiency of 70.3% has been targeted, the reduced number of FIR filter taps as well as the impact of the combined optical and wireless transmission of the generated waveform have yielded a practical sub-optimal efficiency of only 63.6%.

In [14], a non-linear genetic algorithm has been employed to optimize the coefficients of the FIR filter in [7]. As a result, a maximum efficiency of 71% has been achieved using linearly combined sets of higher order pulses of different pulse widths and non-uniform delays. In [15], the number of linearly combined waveforms has been economized to produce an IR-UWB waveform from only two Gaussian doublets. This technique has been further simplified and improved later in [16] to produce an IR-UWB waveform from a linear combination of two monocycles instead of two doublets. Although simple and cost effective, the waveforms reported in [15,16] have achieved efficiencies as low as 12% and 48.52%, respectively.

From the aforementioned overview, it is observed that, reducing the number of linearly combined IR-UWB waveforms inevitably decreases their overall power efficiency. On the other hand, increasing such number, and consequently, the overall efficiency, is limited by several practical implementation issues, such as the fabrication complexity. Moreover, the approaches provided in [13–16] attempt to overcome these performance bounds by economizing the dimensions of the signal space from which linear combinations of IR-UWB waveforms are formed, while maximizing the overall power efficiency of the resulting waveform.

In this paper, the converse approach is followed by maximizing the power efficiency of individual signal space waveforms. The paper contribution is three-fold; (1) A general model of IR-UWB waveform generation is proposed. The model is based on using a single basis function rather than a large number of basis functions. (2) A simplified version of the proposed model is optimized to show the validity as well as the advantages of the proposed design approach. (3) Finally, the obtained results are compared to other related work to emphasize the low-complexity of the proposed approach while providing waveforms with competitive power efficiency.

The rest of this letter is organized as follows. Section 2 presents the proposed IR-UWB waveform generation approach, based on linear combinations of derivatives of an arbitrary basis function. In Section 3, analytical closed-form expressions are developed for the efficiencies of IR-UWB waveforms derived from single order derivatives of Gaussian and sech basis functions. The developed expressions are numerically evaluated and are analyzed in Section 4. Finally, the paper is concluded in Section 5.

## 2. Proposed IR-UWB waveform optimization

In this section, the proposed IR-UWB waveform generation model is explained. The following discussion starts with a general model, followed, in Section 3, by a low-complexity approach that results in an acceptably high power efficiency of IR-UWB waveforms. Fig. 1 illustrates the general model proposed in this paper. This model is inspired from the work provided in [11,17,18].

As shown in this figure, the process of generating a power efficient and FCC compliant IR-UWB waveform is assumed to be divided into two main stages. In the first stage, the differential stage, an input basis function, $\psi(t,\tau)$, having a full width at half maximum (FWHM) pulse width of $\tau$, is simultaneously applied to the inputs of $M$ pulse width modulators. Each of the resulting pulse width modulated waveforms, $\psi(t,\tau\rightarrow\tau_m); m\in 1,2,\ldots,M$, is applied to a time domain differentiator with the proper order before being weighted by a coefficient $\lambda_m\in\Re^+; m\in 1,2,\ldots,M$. The role of the weight coefficient $\lambda_m$ is discussed later in this section. The outputs of the differential stage, $\lambda_m\psi_m(t,\tau_m); m\in 1,2,\ldots,M$, form the signal space member functions from which a linear combination is composed to produce the required IR-UWB waveform, $x(t)$.

Since the spectra of the resulting signal space member waveforms are not fully compliant to the FCC spectral constraints, the differential stage is cascaded by the second stage, which is the spectral shaping output stage. Due to its multiple input–single output (MISO) topology, the second stage is similar to the distributed waveform generator (DWG) reported in [18]. The output combination of this stage is mathematically expressed as follows:

$$x(t)=\sum_{m=1}^{M}\alpha_m\beta_m\lambda_m\psi_m(t-T_m,\tau_m) \tag{1}$$

where $\alpha_m\in\Re$ is the $m$th tap coefficient of the FCC spectral shaping filter, $T_m\in\Re^+$ is its associated delay and $\beta_m\in 0,1$ is a binary valued selection coefficient that controls the coupling/decoupling of a particular signal space member waveform to the relevant tap in the spectral shaping output stage. The sets $\beta_m,\alpha_m$ and $T_m$ should be optimized such that the power efficiency of $x(t)$ is maximized, while complying with the FCC imposed spectral characteristics. In the following, the input basis function, $\psi(t,\tau)$, is either a Gaussian or a sech basis function and is given by

$$\underset{-\infty\le t\le\infty}{\psi(t,\tau)}=\begin{cases}\exp\left(-\dfrac{t^2}{\tau_g^2}\right) & ;\text{ for Gaussian pulses}\\[2ex] \operatorname{sech}\left(\dfrac{t}{\tau_s}\right) & ;\text{ for sech pulses}\end{cases} \tag{2}$$

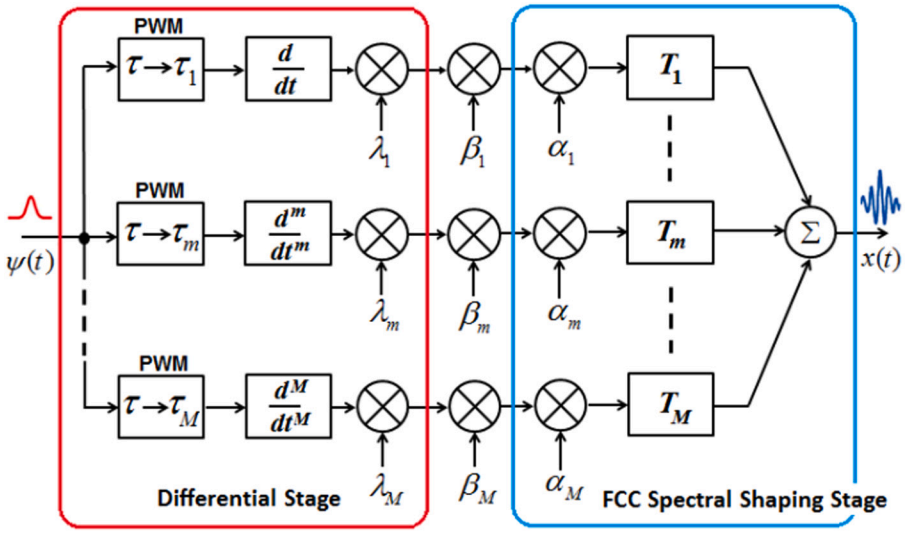


**Fig. 1.** Block diagram representation of the typical stages of the IR-UWB waveform generation process. The design of the differential stage is the subject of this paper. PWM: Pulse width modulator.

where $\tau_g$ is the Gaussian pulse width, defined as the $e^{-1}$ point of the Gaussian basis function. Similarly, $\tau_s$ is the pulse width of the sech basis function. The relationships of $\tau_g$ and $\tau_s$ to $\tau$ guarantees that the Gaussian and the sech basis functions have a common FWHM pulse width of $\tau$. The spectrum of the basis functions in Eq. (2) can be expressed as:

$$\underset{-\infty\le\omega\le\infty}{\Psi(j\omega,\tau)} = \begin{cases} \tau_g\sqrt{\pi}\,\exp\left(-\left(\dfrac{\omega\tau_g}{2}\right)^2\right) & ;\ \text{Gaussian} \\ 4\pi\tau_s\,\operatorname{sech}(2\pi\omega\tau_s) & ;\ \text{sech} \end{cases} \tag{3}$$

Obviously, the generality of the proposed technique guarantees a customizable IR-UWB waveform generator as it allows including an arbitrary linear combination of $M$ signal space member waveforms, with each having an arbitrary and distinct amplitude, pulse width, delay and derivative order. According to Eq. (1), the spectrum of the IR-UWB waveform can be expressed as

$$X(j\omega) = \sum_{m=1}^{M} \alpha_m\beta_m\lambda_m\Psi_m(j\omega,\tau_m)\exp\left(-j\omega T_m\right). \tag{4}$$

Since $\psi_m(t,\tau_m)$ is the $m$th derivative of $\psi(t,\tau_m)$, then $\Psi_m(j\omega,\tau_m) = \mathcal{F}\{\psi_m(t,\tau_m)\} = (j\omega)^m\Psi(j\omega,\tau_m)$. The power spectral density (PSD) of $x(t)$ can be then expressed as

$$\begin{aligned} |X(j\omega)|^2 = &\sum_{m=1}^{M} \beta_m\alpha_m^2\left|\tilde{\lambda}_m\right|^2\left|\Psi_m\left(j\omega,\tau_m\right)\right|^2 \\ &+ \sum_{m=1}^{M}\sum_{n=m+1}^{M} 2\alpha_m\alpha_n\beta_m\beta_n \\ &\times \Re e\left\{\tilde{\lambda}_m\Psi_0\left(j\omega,\tau_m\right)\times\tilde{\lambda}_n\Psi_0\left(j\omega,\tau_n\right)\right\} \end{aligned} \tag{5}$$

where $\tilde{\lambda}_m \triangleq \lambda_m\exp\left(-j\left(\omega T_m - \dfrac{m\pi}{2}\right)\right)$.

According to [11], the power efficiency of the output IR-UWB waveform is given by

$$\zeta_x = \frac{\int_\omega |X(j\omega)|^2 d\omega}{\int_\omega S_{FCC}(\omega)d\omega} = \frac{\int_\omega |X(j\omega)|^2 d\omega}{P_{FCC}} \tag{6}$$

where $S_{FCC}(\omega)$ is the FCC spectral mask. Substituting Eq. (5) into Eq. (6) results in

$$\begin{aligned}\zeta_x &= \sum_{m=1}^{M} \beta_m \alpha_m^2 \chi_m \varphi_m \\ &+ 2\sum_{m=1}^{M}\sum_{n=m+1}^{M} \beta_m \beta_n \alpha_m^2 \alpha_n^2 \chi_{mn} \varphi_{mn}\left(T_m, T_n\right) \\ &= \sum_{m=1}^{M} \beta_m \alpha_m^2 \zeta_{\Psi,m} + 2\sum_{m=1}^{M}\sum_{n=m+1}^{M} \beta_{mn} \alpha_{mn}^2 \zeta_{\Psi,mn}\end{aligned} \tag{7}$$

where $\alpha_{mn} = \alpha_m \alpha_n$, $\beta_{mn} = \beta_m \beta_n$, and where $\zeta_{\Psi,mn} = \chi_{mn}\varphi_{mn}\left(T_m, T_n\right)$ in which $\chi_{mn} = \lambda_m \lambda_n$ and $\varphi_{mn}\left(T_m, T_n\right)$ is given by

$$\begin{aligned}\varphi_{mn}\left(T_m, T_n\right) &= \frac{1}{P_{FCC}} \int_{\omega} \omega^{m+n} \Psi_0\left(j\omega, \tau_m\right) \\ &\times \Psi_0\left(j\omega, \tau_n\right) \cos\left(\omega\left(T_m - T_n\right) + (n-m)\frac{\pi}{2}\right) d\omega\end{aligned} \tag{8}$$

For the terms in which $m = n$, $\chi_{mn} \Rightarrow \chi_m = \left|\tilde{\lambda}_m\right|^2 = \lambda_m^2$ and $\varphi_{mn} \Rightarrow \varphi_m$, resulting in $\zeta_{\Psi,m} = \chi_m \varphi_m$.

## 3. Optimal signal space waveforms

In this section, the model proposed in the previous section is used to obtain power efficient low-complexity IR-UWB waveforms. From Eq. (7), it can be conjectured that the IR-UWB waveform, $x(t)$, can be partially optimized by optimizing the power efficiencies, $\zeta_{\Psi,m}$, of each of the $M$ individual signal space components. An optimal design for the waveform $x(t)$ would be obtained by maximizing $\zeta_x$ through finding the optimum values of $\lambda_m, \alpha_m, \beta_m$ and $T_m$ while maintaining the FCC regulations such that $|X(j\omega)|^2 \le S_{FCC}(\omega) \quad \forall\omega$. While the maximum of $|X(j\omega)|^2$ can be set to $\max S_{FCC}(\omega)$ to achieve high power efficiency, the FCC spectral shaping stage in Fig. 1 is essential to fulfill FCC compliance at all frequencies. This can be achieved through pulse shaping techniques such as the circuit designs presented in [17,18]. In the following, a sub-optimal approach is followed to obtain an FCC-compliant waveform with low generation complexity.

The main idea is to ensure that $\max\left\{|X(j\omega)|^2\right\} = \max\left\{S_{FCC}(\omega)\right\}$ within the range of frequency on interest. It is assumed that the dimensionality of the signal space is reduced to a single waveform of an arbitrary derivative order $m$. Accordingly, $\chi_m$ is set to $\dfrac{\max\left\{S_{FCC}(\omega)\right\}}{\max\left\{\left|\Psi_m(j\omega,\tau)\right|^2\right\}}$. The peak PSDs of Gaussian-based and sech-based derivatives are obtained by determining the proper basis function and solving

$$\frac{\partial}{\partial\omega}\left|\Psi_m(j\omega,\tau)\right|^2 = 0 \tag{9}$$

to obtain the frequency, $\omega^*$, for which the derivative pulse is maximized. For the $m$th order Gaussian-based IR-UWB waveforms, the peak PSD frequency, $\omega_g^*$, is given by [6]

$$\omega_g^* = \frac{\sqrt{2m}}{\tau_g}. \tag{10}$$

On the other hand, for the $m$th order sech-based IR-UWB waveform, the peak of the PSD occurs at $\omega_s^*$ that can be obtained through the numerical solution of

$$\left(2\pi\omega_s^*\tau_s\right) = \frac{m}{\tanh\left(2\pi\omega_s^*\tau_s\right)} \tag{11}$$

Consequently, The corresponding values, $\chi_m|_g$ and $\chi_m|_s$, are obtained, for Gaussian-based and sech-based IR-UWB waveforms, respectively, as follows:

$$\chi_m|_g = \max\left\{S_{FCC}(\omega)\right\} \frac{\exp\left(\left(\omega_g^*\tau_g\right)^2\right)}{2\left(\left(\omega_g^*\right)^{2m}\pi\tau_g^2\right)} \tag{12}$$

and

$$\chi_m|_s = \max\left\{S_{FCC}(\omega)\right\} \frac{\cosh^2\left(2\pi\omega_s^*\tau_s\right)}{\left(\left(\omega_s^*\right)^{2m}\left(4\pi\tau_s\right)^2\right)}. \tag{13}$$

It can be seen from Eqs. (12) and (13) that, tuning the pulse width of the input basis function should be accompanied by a corresponding variation in its amplitude, with the pulse width as the key controllable parameter, such that a maximum PSD

of $\max\{S_{FCC}(\omega)\}$ is always guaranteed for each individual waveform component in the signal space. The power efficiencies of Gaussian-based IR-UWB waveforms, $\zeta_m|_g$ are obtained as follows:

$$\begin{aligned}\zeta_m|_g &= \frac{(\pi\tau_g)^2}{\Omega G_p}\int_{\omega_L}^{\omega_H}\omega^{2m}\exp\left(-\frac{(\omega\tau_g)^2}{2}\right)d\omega \\ &= \left(\frac{\pi^2 2^{\frac{m+1}{2}}}{\Omega G_p \tau_g^{m-1}}\right)\left(\Phi_m\left(\frac{\omega_H\tau_g}{\sqrt{2}}\right)-\Phi_m\left(\frac{\omega_L\tau_g}{\sqrt{2}}\right)\right)\end{aligned} \tag{14}$$

where $\omega_H$ and $\omega_L$ are the highest and the lowest frequencies, respectively, and where $\Omega = \omega_H - \omega_L$. The term $G_p$ is defined as $G_p = \left(\left(\omega_g^*\right)^{2m}\pi\tau_g^2\right)\exp\left(-\left(\omega_g^*\tau_g\right)^2/2\right)$, and the term $\Phi_m(u)$ is given by

$$\begin{aligned}\Phi_m(u) &= (1-s)\Gamma\left(\frac{m+s+1}{2}\right)\mathrm{erf}(u) \\ &\quad - \exp\left(-u^2\right)\sum_{n=0}^{L-1}\frac{\Gamma\left(\frac{m+1}{2}\right)}{\Gamma\left(\frac{m+1}{2}-n\right)}u^{m-2n-1}\end{aligned} \tag{15}$$

where $L = \frac{m+s}{2}$ with $s = 0$ for odd values of $m$, while $s = 1$ for even values of $m$. The gamma function, $\Gamma(z)$, and the Gaussian error function, $\mathrm{erf}(z)$, are given respectively, by

$$\begin{aligned}\Gamma(z) &= \int_{x=0}^{\infty} y^{z-1}\exp(-y)\quad dy \\ \mathrm{erf}(z) &= \frac{2}{\sqrt{\pi}}\int_0^z \exp\left(-y^2\right)\quad dy\end{aligned} \tag{16}$$

Similarly, for sech-based IR-UWB waveforms, the power efficiency $\zeta_m|_s$ is obtained as

$$\begin{aligned}\zeta_m|_s &= \frac{(4\pi\tau_s)^2}{\Omega S_p}\int_{\omega_L}^{\omega_H}\omega^{2m}\,\mathrm{sech}^2\left(2\pi\omega\tau_s\right)d\omega \\ &= \left(\frac{m!\pi^{m-1}2^{6-m}}{\Omega S_p\tau_s^{m-1}}\right)\left[\Pi_m\left(2\pi\omega_H\tau_s\right)-\Pi_m\left(2\pi\omega_L\tau_s\right)\right]\end{aligned} \tag{17}$$

where $S_p = \left(4\pi\tau_s\left(\omega_s^*\right)^m\right)^2\mathrm{sech}^2\left(2\pi\omega_s^*\tau_s\right)$ and $\Pi_m(u)$ is given by:

$$\Pi_m(u) = \sum_{l=0}^{\infty}\sum_{q=0}^{m}\frac{(-1)^{l+q}(l+1)u^{m-q}}{(m-q)!(-2(l+1))^{q+1}}e^{-2(l+1)u} \tag{18}$$

The terms $\Pi_m(\cdot)$ in Eq. (17) are calculated numerically through truncating the expression in Eq. (18). However, due to the rapid decay of the summands as $l$ increases, the accuracy of $\Pi_m(\cdot)$ becomes essentially independent of the upper limit of $l$ for $l > 10$.

## 4. Analytical and numerical results

In this section, numerical examples are provided to show the validity and effectiveness of the proposed waveform generation approach. In the following, the FCC UWB mask in [1] is considered such that, $\max\{S_{FCC}(\omega)\} = -41.3$ dBm/MHz in the range from $\omega_L = 2\pi\times 3.1$ G rad/s to $\omega_H = 2\pi\times 10.6$ G rad/s.

The first set of results are shown in Fig. 2, where the power efficiency in Eq. (7) is calculated at different values of the pulse widths, $\tau_g$ in the case of Gaussian pulses and $\tau_s$ in the case of sech pulses. In each case, the peak emission angular frequencies in Eqs. (11) and (12) are calculated for each waveform type and each order $m \in \{1, 2, \ldots, 7\}$. The obtained frequencies are then substituted into Eqs. (14) and (17) to evaluate the power efficiencies for Gaussian-based and sech-based pulses, respectively.

The results in Fig. 2 show that there is an optimum pulse width, $\tau_g$ or $\tau_s$, at which a global maximum of the power efficiency is obtained. This pulse width changes with the change of the derivative order of the basis pulse. For example, for the monocycle Gaussian basis waveform, a peak power efficiency of 83.15% is achieved at a pulse width of $\tau_g = 50.51$ ps, while for the monocycle sech basis waveform, a peak power efficiency of 86.6% is achieved at a pulse width of $\tau_s = 11.32$ ps.

It can be also observed that the higher the derivative order of the basis function, the lower the peak power efficiency and the larger the pulse width that the peak occurs at. For example, in the case of sech basis waveform, while a peak power efficiency of 70% occurs at $\tau_s = 38$ ps for the 4th order derivative, a lower peak power efficiency of 60% occurs at $\tau_s = 62$ ps for the 7th order derivative.

It is noteworthy that such small pulse widths, in the picoseconds range, are challenging in practical implementation. However, there have been vast interest in both research and industry to implement such narrow pulses. For example, the authors in [19] used the model 3500D impulse generator of Picosecond Pulse Labs that produces fast impulses with a FWHM of about 75 ps. In addition, many attempts have been made to design IR-UWB pulse generators. In [20], the authors introduce a tunable IR-UWB pulse generator based on feedback oscillator switching that can be used to generate pulses with pulse width tuning range of $1 \sim 6.5$ ns. In

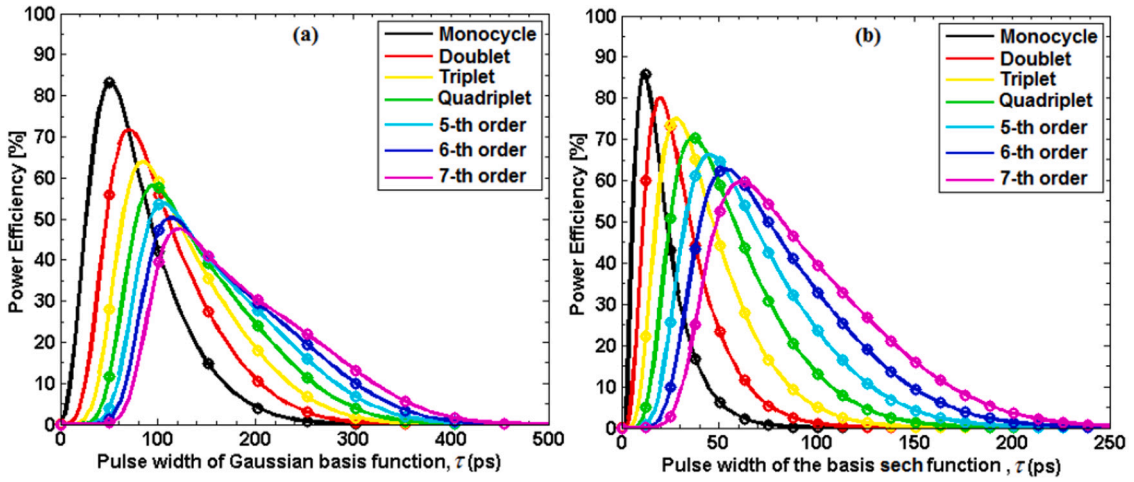


**Fig. 2.** The waveform power efficiency versus with the FWHM pulse width of single order derivatives of IR-UWB waveforms (a): Gaussian Waveform and (b) Sech Waveform.

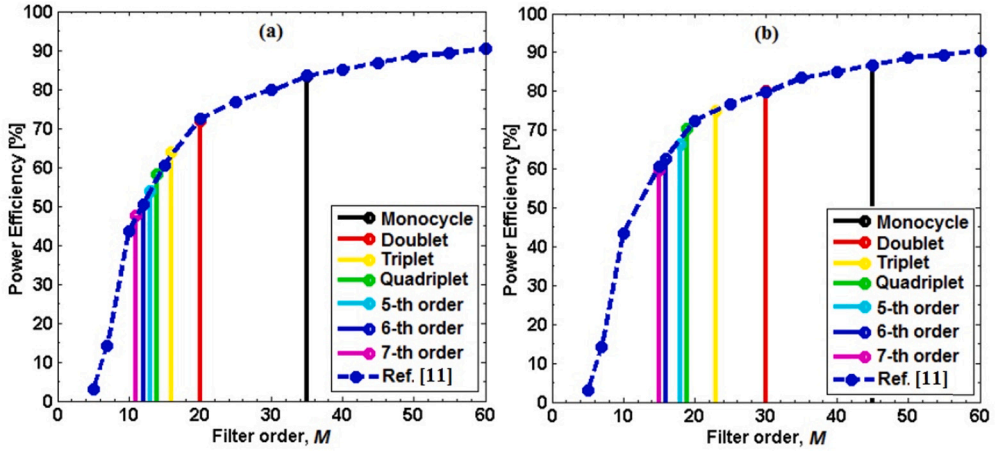


**Fig. 3.** The waveform power efficiency of $m$th order derivatives with optimized FWHM pulse width for the cases of IR-UWB waveforms (a): Gaussian Waveform and (b) Sech Waveform. The case of a linear combinations of $M$ orthogonal monocycle pulses (from [11]) is shown for comparison.

a relatively older work, the authors in [21] proposed and implemented an IR-UWB pulse generator architecture, based on 0.18 μm CMOS technology to generate pulses of 0.5 ns width. The authors later implemented another architecture for tunable spectrum in [22], resulting in pulses of 0.6 ns width. In [23], the authors propose an adaptive pulse generator using PAM to produce pulses at mean central frequency ∼ 3.7 GHz, of mean pulse duration ∼ 270 ps. With advances in technology, and driven by needs such those highlighted in these results, researchers are capable of designing narrower width pulse generators.

The second set of results show the peak power efficiencies, obtained at the optimum FWHM pulse width, for a single $m$th order derivative of either a Gaussian basis waveform or a sech basis waveform. Note that when a single $m$th order derivative pulse is used, rather than $M$ derivatives, the expression of the IR-UWB spectrum waveform will follow from Eq. (4) as

$$X(j\omega) = \underbrace{\lambda_m \Psi_m(j\omega, \tau_m)}_{\text{Differential stage}} \quad \underbrace{\alpha_m \exp\left(-j\omega T_m\right)}_{\text{FCC pulse shaping stage}} . \tag{19}$$

In order to show the effectiveness of the proposed approach, the power efficiencies obtained through the proposed approach are compared to those obtained through an optimized linear combination of FIR filtered Gaussian pulses of [11]. The results are presented in Fig. 3.

It can be seen from Fig. 3 that the proposed waveform generation method can be used to result in desired power efficiency with much simpler generation method, and without need for a large number of FIR filtered pulses. For example, a *single* Gaussian monocycle with optimized pulse width, as proposed in this work, results in a power efficiency around 83.15% which is not achieved, according to the approach in [11], except with 33 or more linearly combined Gaussian pulses. Note that, with 10 linearly combined

monocycles, the approach in [11] results in an efficiency around 45%, less than that obtained by a single 7th order derivative pulse with optimized pulse width.

Similarly, with a sech basis waveform, a second order derivative with optimized pulse width will result in a power efficiency of 80%. On the other hand, 30 linearly combined monocycles of Gaussian pulses are needed to achieve similar efficiency. This emphasizes the advantage of the proposed approach in obtaining high power efficiency through much less complex and easier generation approach. Extending the proposed approach to a linear combination of optimized $m^th$ order derivatives is promising to achieve a required efficiency with much less number of component waveforms compared to approached in [11–16].

## 5. Conclusion

In this paper, a low-complexity approach is proposed to generate power efficient impulse radio ultra-wide band waveforms, based on linear combinations of IR-UWB waveforms derived from Gaussian or sech basis functions. Accurate closed-form analytical expressions were developed for the power efficiencies of the combined waveforms. Such expressions are useful in the design and the development of practical, low-complexity IR-UWB waveform generators, based on finite impulse response filters. Special cases, in which a single derivative component of the basis waveform, are studied. In such cases, the pulse width is optimized for the maximum power efficiency. Comparisons to other approaches show that the proposed approach, although of low-complexity, yet it can provide similar or higher power efficiencies than other high-complexity approaches.

## Declaration of competing interest

The authors declare that they have no known competing financial interests or personal relationships that could have appeared to influence the work reported in this paper.

## Acknowledgments

This work was supported by the Egyptian National Telecom Regulatory Authority (NTRA).

## References

[1] US. Fed. Comm. Commission First Report and Order, Revision of part 15 of the commission's rules regarding ultra wideband transmission systems, Tech. Rep., 2011.
[2] Y. Yue, H. Huangand, L. Zhangand, J. Wangand, J.-Y. Yang, O.F. Yilmazand, J.S. Levyand, M. Lipson, A.E. Willner, UWB monocycle pulse generation using two-photon absorption in a silicon waveguide, Opt. Lett. 37 (2012) 551–553.
[3] H. Chen, M. Chen, J. Zhang, S. Xie, UWB monocycle and doublet pulses generation in optical domain, IEEE Photonics J. 6 (2014) 1–7.
[4] A. Naji, P. Warr, M. Beach, K. Morris, A fundamental limit on the performance of geometrically-tuned planar resonators, IEEE J. Lightwave Technol. 26 (2008) 628–635.
[5] D.M. Pozar, Waveform optimizations for ultrawideband radio systems, IEEE Trans. Antennas Propag. 51 (2003) 2335–2345.
[6] D.M. Pozar, Optimal radiated waveforms from an arbitrary UWB antenna, IEEE Trans. Antennas Propag. 51 (2007) 3384–3390.
[7] L. Gingras, W. Cui, A.W. Schiff-Kearn, J.-M. Ménard, A.G. Cooke, Active phase control of terahertz pulses using a dynamic waveguide, Opt. Express 26 (2018) 13876–13882.
[8] A. Zadok, X. Wu, J. Sendowski, A. Yariv, A.E. Willner, Reconfigurable generation of high-order ultra-wideband waveforms using edge detection, J. Lightwave Technol. 28 (16) (2010) 2207–2212.
[9] G. Avdeenko, T. Narytnyk, V. Korsun, V. Saiko, Simulation of a Terahertz band wireless telecommunication system based on the use of IR-UWB signals, Telecommun. Radio Eng. 78 (2019) 901–919.
[10] M.D. Di Benedetto, B. Vojcic, Ultra-wideband wireless communications: A tutorial, J. Commun. Netw. 5 (2003) 290–302.
[11] X. Wu, Z. Tian, T.N. Davidson, G.B. Giannakis, Optimal waveform design for UWB radios, IEEE Trans. Signal Process. 54 (2006) 2009–2021.
[12] M. Abtahi, J. Magne, M. Mirshafiei, L. Rusch, S. LaRochelle, Generation of power-efficient FCC-compliant UWB waveforms using FBGs: Analysis and experiment, Lightwave Technol. 26 (2008) 628–635.
[13] M. Abtahi, M. Mirshafiei, S. LaRochelle, L. Rusch, All-optical 500-Mb/s UWB transceiver: An experimental demonstration, Lightwave Technol. 26 (2008) 2795–2802.
[14] M. Mirshafiei, M. Abtahi, P. Larochelle, L. Rusch, Pulse shapes that outperform traditional UWB antenna/waveform combinations, in: Global Telecommunications Conference (GLOBECOM 2010), 2010 IEEE, 2010, pp. 1–5.
[15] S.T. Abraha, C.M. Okonkwo, E. Tangdiongga, A.M.J. Koonen, Power-efficient impulse radio ultrawideband pulse generator based on the linear sum of modified doublet pulses, Opt. Lett. 36 (2011) 2363–2365.
[16] S.T. Abraha, C. Okonkwo, H. Yang, D. Visani, Y. Shi, H.-D. Jung, E. Tangdiongga, T. Koonen, Performance evaluation of IR-UWB in short-range fiber communication using linear combination of monocycles, Lightwave Technol. 29 (2011) 1143–1151.
[17] D. Barras, W. Hirt, H. Jackel, A spectrum-shaping output stage for IR-UWB transmitters, IEEE Trans. Microw. Theory Tech. 57 (2009) 1470–1478.
[18] Y. Zhu, J.D. Zuegel, J.R. Marciante, H. Wu, Distributed waveform generator: A new circuit technique for ultra-wideband pulse generation, shaping and modulation, IEEE J. Solid-State Circuits 44 (2009) 808–823.
[19] X. Zeng, A. Fhager, P. Linner, M. Persson, H. Zirath, Experimental investigation of the accuracy of an ultrawideband time-domain microwave-tomographic system, IEEE Trans. Instrum. Meas. 60 (12) (2011) 3939–3949.
[20] L. Šneler, T. Matić, M. Herceg, A tunable CMOS IR-UWB pulse generator based on feedback controlled oscillator switching, IEEE Trans. Circuits Syst. II 68 (6) (2021) 1902–1906.
[21] J. Radic, A. Djugova, L. Nagy, M. Videnovic-Misic, New design of low power, 100Mb-s IR-UWB pulse generator in 0.18μm CMOS technology, Microelectron. J. 44 (12) (2013) 1215–1222.
[22] J. Radic, M. Brkic, A. Djugova, M. Videnovic-Misic, B. Goll, H. Zimmermann, Ultra low power low complexity 3-7.5 GHz IR-UWB transmitter with spectrum tunalbility, IET Circuits, Dev. Syst. 14 (2020) 521–527.
[23] L.C. Moreira, J.F. Neto, W.S. Oliveira, T. Ferauche, G. Heck, N.L.V. Calazans, F.G. Moraes, An IR-UWB pulse generator using PAM modulation with adaptive PSD in 130 nm CMOS process, in: Proceedings of the 32nd Symposium on Integrated Circuits and Systems Design, Association for Computing Machinery, 2019, pp. 1–6.